applied sciences

MDPI

Article

Versatile High-Throughput Platform for Focused Ultrasound In Vitro Application

Steffen H. Tretbar [1,2,*], Marc Fournelle [1], Christian Degel [1], Franz-Josef Becker [1], Peter Weber [1], Sarah Therre-Mohr [1,3], Wolfgang Bost [1], Lisa Landgraf [2] and Andreas Melzer [2,4]

[1] Department Ultrasound, Fraunhofer Institute for Biomedical Engineering IBMT, 66280 Sulzbach, Germany; marc.fournelle@ibmt.fraunhofer.de (M.F.); christian.degel@ibmt.fraunhofer.de (C.D.); franz.josef.becker@ibmt.fraunhofer.de (F.-J.B.); peter.weber@ibmt.fraunhofer.de (P.W.); sarah.therre-mohr@ibmt.fraunhofer.de (S.T.-M.); wolfgang.bost@ibmt.fraunhofer.de (W.B.)
[2] Innovation Center Computer Assisted Surgery, Faculty of Medicine, University of Leipzig, 04103 Leipzig, Germany; andreas.melzer@uni-leipzig.de (A.M.)
[3] Department of Molecular and Cellular Biotechnology, Saarland University, 66123 Saarbruecken, Germany
[4] Institute for Medical Science & Technology IMSaT, University of Dundee, Dundee DD1 4HN, UK
* Correspondence: steffen.tretbar@ibmt.fraunhofer.de; Tel.: +49-6897-9071-300

Abstract: For the more efficient application of ultrasound in future therapies, fundamental research is needed on the mode of action of ultrasound on biological systems using therapeutic frequencies. To address this need, a new versatile high-throughput platform for focused ultrasound in vitro application was designed, developed, and characterized. The applicator was aligned with the dimensions of a 96-well plate and frequencies commonly used in the therapeutic ultrasound range (0.5–2.0 MHz). Two different platform configurations were developed: (a) a low-intensity version with 96 individual transducers allowing dry coupling of the well plate; and (b) a high-intensity version with water cooling, supporting parallel sonication of 32 out of 96 wells. The platforms were characterized by performing an analysis of the homogeneity of the sound pressure and intensity, the impact of filled volume per well, the cross-coupling effect between the wells, and the influence of the well plate. The low-intensity design delivers pressure levels up to 605 kPa inside the well with maximum I_{SPPA} values between 0.78 and 12.38 W/cm^2. In contrast, the high-intensity system achieves pressures up to 1460 kPa and a maximum I_{SPPA} of 72 W/cm^2 inside the wells. The successfully developed high-throughput platform supports parallelized sonication in standard, well-plate formats and is suitable for focused ultrasound applications in vitro.

Keywords: high-intensity focused ultrasound; in vitro setup; low-intensity focused ultrasound; therapeutic ultrasound; versatile high-throughput platform

Academic Editor: Garoli Denis

Received: 29 November 2024
Revised: 10 January 2025
Accepted: 13 January 2025
Published: 16 January 2025

Citation: Tretbar, S.H.; Fournelle, M.; Degel, C.; Becker, F.-J.; Weber, P.; Therre-Mohr, S.; Bost, W.; Landgraf, L.; Melzer, A. Versatile High-Throughput Platform for Focused Ultrasound In Vitro Application. *Appl. Sci.* **2025**, *15*, 847. https://doi.org/10.3390/app15020847

1. Introduction

Ultrasound (US) has emerged as a prominent non-invasive therapeutic modality over recent years. There are 166 clinical indications that are being studied and treated with focused ultrasound (FUS) systems, which are in various stages of development [1]. Applications range from tumor therapy [2–4], neurodegenerative [5,6] and psychiatric diseases [7], movement disorders [8,9], pain [10], and stroke treatment [11,12] to Alzheimer's disease [13]. For therapy of the above-named conditions, different ultrasound effects have been investigated, ranging from thermal ablation, mechanical fragmentation, (mild) hyperthermia, blood–brain barrier (BBB) opening, or targeted drug delivery (TDD) to ultrasound neuromodulation. A common point in all these applications is that the

ultrasound parameters, in particular, the frequency, the pressure, and the intensity, have a great impact on the resulting effect. In processes in which no irreversible effect on tissues is desired, such as BBB-opening, TDD or neuromodulation, the pressure and intensity have to be carefully adjusted such that there is no thermal or mechanical damage to the cells. On the other hand, ideal sonication parameters leading to the desired effect (e.g., transient BBB opening) with a high level of certainty are sometimes still unclear and need further investigation. Accordingly, to expand the field of application of FUS, new ultrasound therapy systems must be developed, and parameters that ensure the best therapeutic effect and outcome must be identified. While clinical translation is already ongoing in some fields, further pre-clinical work is needed in many ultrasound applications. For this purpose, in vitro studies are the preferred method of choice [14,15], especially at an early stage of research and when statistical significance is sought, which can be achieved by parallelized cell model experiments more easily than on small animal models. However, there is a lack of ultrasound systems optimized for research into FUS effects on cell models which allows for a variation in crucial sonication parameters (e.g., sound pressure, frequency, modulation sequence). Current setups mostly rely on single-element transducers optimized for a defined spectral and pressure range, which are not adapted for high-throughput (HTP) cell culture workflows. In the past, setups for in vitro treatment have often been based on single transducer systems that were immersed, e.g., in a petri dish [16,17]. However, this direct contact with the cell medium is a major disadvantage in terms of contamination and influence on the cell models. It requires intensive cleaning and sterilization efforts before and between studies and, furthermore, alters the cell environment even without actually applying ultrasound (just by immersing transducers in the medium).

Further systems have been described in which water is used as a coupling medium and where a single FUS transducer is positioned in a bath below the cell medium. Such systems have been used for sonication in standard multi-well plates [18,19], customized bioreactors [20], or single-cell culture dishes [21]. However, since only one US transducer is available, even when using a multi-well setup, only one experiment can be performed at a time, and statistical significance is hard to achieve.

Multi-element US arrays initially designed and developed for clinical settings, in which the ultrasound focus is applied to the individual wells from the bottom of a water bath [22], have also been investigated. Further approaches are based on several (up to 5) US single-element transducers, which need to be mechanically maneuvered in the water bath [23]. Although it has been demonstrated that several wells of multi-well plates can be addressed by such systems, the very high costs [22] and the complexity [23] prevent the use of the routine tool in the research on in vitro models. Furthermore, standing waves [24] or undesired cross-coupling from well to well [25] can have an unwanted effect.

To overcome the limitations of the so-far-developed cell sonication systems, we developed a new set of sonication systems optimized for multi-well settings. This paper describes the design, development, and characterization of our new versatile multi-transducer platform for parallel low-intensity-(LIFU) and high-intensity-(HIFU) FUS applications, optimized for investigating the effects of therapeutic ultrasound in in vitro setups.

2. Materials and Methods

2.1. System Requirements

The primary objective of this work was to develop a platform for efficient use in biotechnological HTP workflows for the in vitro investigation of therapeutic ultrasound on cell models. The system should:

1 Enable parallel ultrasound treatment (for instance, by using 96-well plates);

2 Have transducer focal diameters adapted to the size of the single wells (6.58 mm in diameter, 9.0 mm distance between individual wells);
3 Provide adjustable output sound pressure (p_{max}) of at least >100 kPa inside the wells, with a large homogeneity over all wells;
4 Support sonication over a frequency range typical for therapeutic ultrasound (0.5–2.0 MHz) and avoid cross-coupling of the sound into an adjoining well;
5 Facilitate dry-coupling of the well plate and offer ease of handling for HTP experiments under sterile conditions of the in vitro models.

2.2. Simulation of Different Platform Configurations

The configuration of the well applicator and the design of the individual transducers were made as a compromise between constraints relating to the mechanical setup (e.g., usage of 96-well plates, where all wells can be sonicated individually or simultaneously) or relating to the acoustical output (e.g., I_{SPTA} as high as possible). Two concepts were pursued in this work: A low-intensity and a high-intensity focused ultrasound platform. For the design of the transducer, simulations were performed either using the in-house developed simulation tool SCALP based on point source synthesis or FEM simulations were performed using PZFlex V. 1.25.3.0 (Onscale Inc., Redwood City, CA 94063, USA).

2.2.1. Low Intensity Focused Ultrasound (LIFU) Platform

The main requirement for the LIFU platform was the ability to sonicate all 96 wells of the multi-well plate in parallel, using a single transducer for each well. Accordingly, the pitch of the well applicator was given by one of the multi-well plates (9 mm), and the size of the individual transducers was determined by the individual well diameter (6.58 mm). The remaining design choices were associated with the thickness and the material (PZT or piezo composite) of the piezoceramic layer. For the design of the piezo composite, different configurations with varying rod sizes (lateral) and kerfs were initially simulated in PZFlex V. 1.25.3.0 (Onscale, ANSYS, Inc., Redwood City, CA, USA) and compared with the behavior of bulk PZT. The simulations were limited to individual transducers because there was no overlap of the pressure fields in the final set-up design, with air-filled walls separating different wells.

The simulations shown in Figure 1 were performed in a free field and, therefore, only partially represent the final setup with wells filled to a defined target level. Nevertheless, they confirmed that the lateral spread of the sound field (relative to the aperture, which corresponded to the placement of the well) did not exceed the well diameter, indicating that most of the acoustic energy was applied to the well. However, it was evident in the simulations that with this small aperture diameter, the sound field maxima at the different operating frequencies were at different depths. According to the simulations, only the 0.5 and 1 MHz versions showed axial focus positions within a well depth of 10.9 mm.

2.2.2. High-Intensity Focused Ultrasound (HIFU) Platform

The HIFU platform was designed to facilitate the application of higher pressures and extended duty cycles in the wells. Because the high-pressure levels required to study effects beyond mild hyperthermia pose significant challenges to individual transducers for each well in a 96-well plate, subset configurations of the plate were studied that could be effectively sonicated simultaneously. To compromise between high pressure and stimulating as many wells as possible, a configuration of 8 × 4 cylindrically focusing transducers was chosen. The dimension along the short side of one element (labeled x-dimension in Figure 2a) corresponded to that of one well, while the dimension of the long side (labeled y-dimension in Figure 2a) corresponded to the size of three wells (Figure 2a,b).

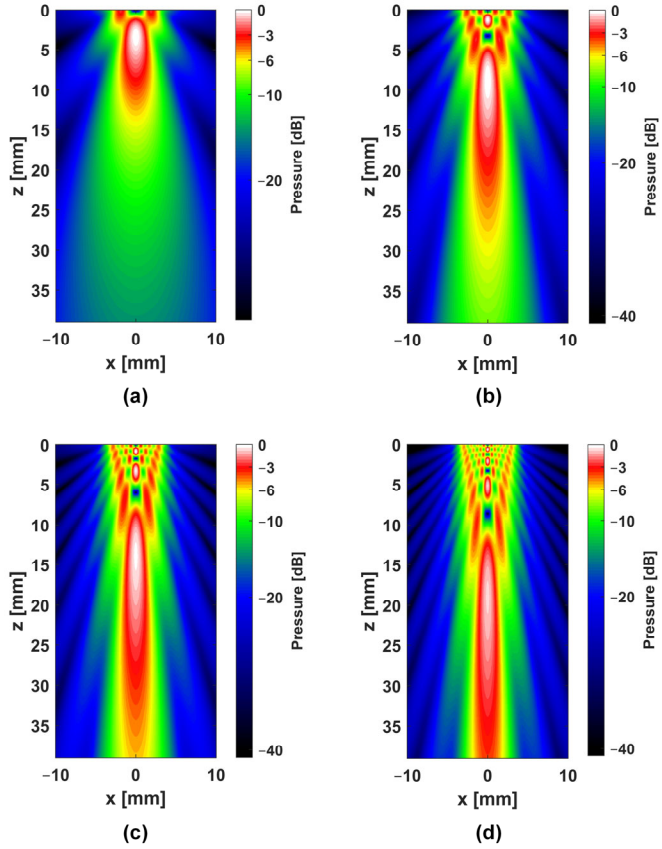

Figure 1. Simulated XZ pressure distribution field for different circular single-element LIFU transducers of diameter 6.5 mm and frequencies 0.5 MHz (**a**), 1.0 MHz (**b**), 1.5 MHz (**c**) and 2.0 MHz (**d**).

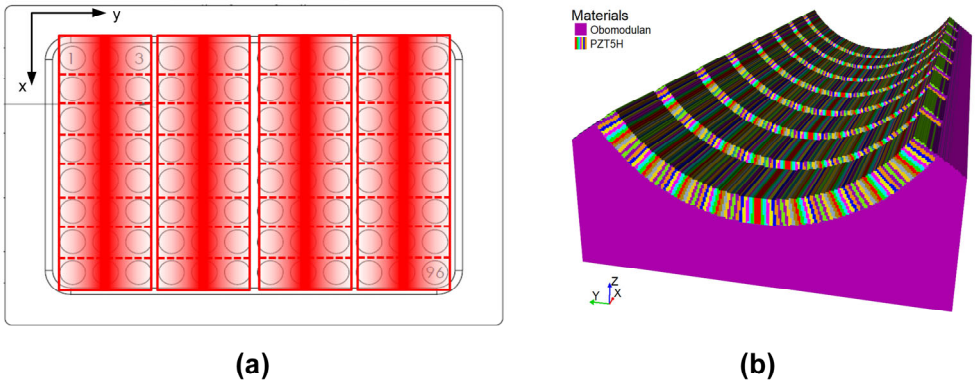

Figure 2. Applicator geometry with 32 cylindrically focusing transducers for sonication in 32 wells of a 96-well plate. (**a**) Projection of acoustic pressure distribution is schematically shown as a semi-transparent overlay on the well plate model; (**b**) Model of one stack of 8 focusing transducers used as input for the FEM simulation.

One challenge with this configuration was reducing the overlap of the pressure fields from adjacent elements due to the larger opening angle in the x-dimension. FEM simulations to optimize the geometry were performed on a simplified model (Figure 3) consisting of a stack of eight cylindrical PZT5H ceramic elements with a backing made of a polyurethane material (Obomodulan®, OBO-Werke, Stadthagen, Germany). Initial optimizations on the stack of eight elements led to a coverage angle of 110° for the ceramics with an inner cylinder radius of 13.5 mm and a ceramic thickness of 2 mm. A gap of 2.2 mm between adjacent elements was filled with polyurethane. It was assumed that the transducer elements interface with the well plate via water coupling.

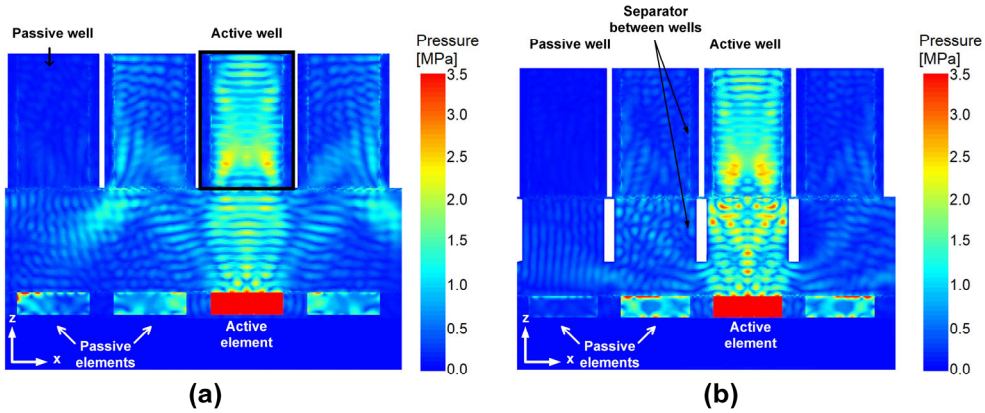

Figure 3. FEM simulation of the acoustic pressure distribution in the XZ dimension when exciting a single element of the 8-element stack with a 1 MHz CW sinus signal. (**a**) Without interelement separator; (**b**) With interelement separator.

In further numeric experiments, we explored the influence of different backing materials (OBO vs. air), piezoceramic materials, and the dimensions of the eight-element stack on the pressure disturbance to refine the configuration. The effect of sound field separators between adjacent transducers to reduce the pressure disturbance is displayed in Figure 3. Of the sound pressure contained in the well above the active transducer, 49% was transmitted to adjacent cells without the presence of separators, whereas this value fell to 30% of the active well when using OBO walls. Due to the requirement for active cooling of the transducer elements when driven at high duty cycles and voltages (determined by thermal simulations), complete acoustic separation in the x-dimension was not possible. A small opening in the separator between adjacent transducers (Figure 3b) allowed the passage of cooling fluid along channels aligned in the x-dimension. The separator (indicated in white) left a gap for water to flow directly above the transducer element surface.

The final specifications for the two applicator configurations are summarized in Table 1.

Table 1. Overview of the technical specifications for the HIFU and LIFU applicator versions.

	LIFU Version	**HIFU Version**
Frequency	0.5/1.0/1.5/2.0 MHz	1.0 MHz
Transducer dimension	D = 6.5 mm	cylindrical
Transducer material	PZT composite	PZT5H
Wells addressed	96	32
Coupling	Polymer	Water
Cooling	Air	Water

LIFU = Low-intensity focused ultrasound, HIFU = High-intensity focused ultrasound, D = diameter.

2.3. Setup

2.3.1. LIFU Platform

Different models of the LIFU applicator were set up using common geometry and configuration. Initially, 6.5 mm cylindrical elements (Figure 4a) were manufactured by milling. Depending on the intended transducer frequency, either a PZT or piezo composite backing material was applied, either as a plate the size of the applicator or as small pieces on an OBO backing using silver epoxy adhesive. Wires were threaded through the backing to establish individual electrode contact with the elements prior to contact with a common ground electrode (Figure 4b). To facilitate air cooling when driven with high duty cycles, spaces between elements were intentionally left void. A polymeric coupling material was applied on top of the ground electrode. Finally, the applicator was integrated into a

3D-printed housing (Figure 4c), and a connector PCB was used to connect the 96 individual wires and the ground electrode to a single BNC cable.

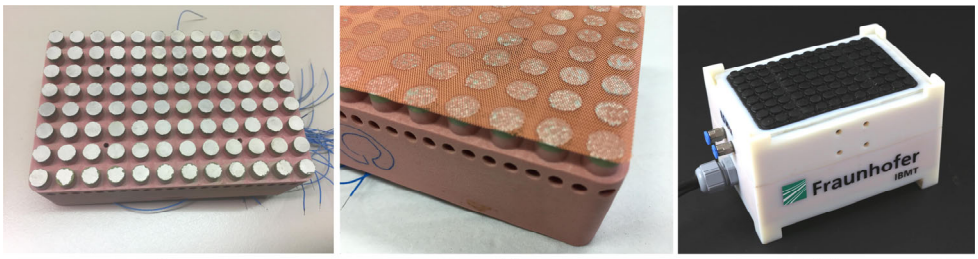

(a) (b) (c)

Figure 4. Setup of the LIFU system. (**a**) Piezo composite/PZT applied to an OBO backing. Individual contacting of the elements by means of drilling through the backing and insertion of contacting wire. Shaping of cylindrical elements by milling of the ceramics; (**b**) Application of the common top grounding electrode; (**c**) Final integration into the housing with a polymeric coupling layer on elements, electric cabling, and air cooling.

2.3.2. HIFU Platform

The HIFU platform, optimized for 1 MHz, features 32 cylindrically focusing PZT elements spanning an angle of 110° with a vertical dimension of 8 mm, a thickness of 2 mm, and an inner radius of 13.5 mm. Initially, contacting cables were soldered to the elements (Figure 5a). Next, an OBO backing was prepared by milling, with holes accommodating the insertion of the contacting cables from the rear, along with milled inter-element OBO separators, which were inserted between adjacent transducers (Figure 5b). The 32 applicator elements were formed from 4 stacks of 8 transducer elements, which were fully interchangeable in case of any defect. A protective insulation layer of epoxy resin was applied to prevent corrosion of the aperture. The 4 stacks were integrated into a housing (Figure 5b,d), which sealed the elements under a polymer membrane. Water cooling channels were built into the applicator housing, aligned along the x-dimension of each stack. A 96-well plate holder was manufactured with mechanical inserts to allow the placement of the applicator in positions for simultaneous sonication of specific well rows (1, 4, 7, 10; 2, 5, 8, 11 or 3, 6, 9, 12). Pressure valves regulated the flow of the cooling medium and controlled the inflation/deflation of the sealing membrane. Acoustic coupling to the wells was achieved via a layer of water on top of the sealing membrane.

2.3.3. Applicator Driving Electronics

A high-power single-channel generator (AG-1016, T&C Power Conversion Systems, Rochester, NY, USA) provided power to the applicators. For the HIFU design, two sub-groups of 16 elements (2 rows) were driven separately, offering customizable parameter settings for well subsets. An impedance matching circuit was included (T1K-7A, T&C Power Conversion Systems, Rochester, NY, USA) for improved driving efficiency. For the HIFU design, an external pump equipped with a heat exchanger (WK 16-1 DS, Colora Messtechnik GmbH, Lorch, Germany) was used to drive the cooling circuit. Sonication parameters (frequency, amplitude, burst count, PRF) can be adjusted directly using the single channel electronics controls or our proprietary software tool “Cell Therapy Planning Tool” V1.0 (Fraunhofer IBMT, Sulzbach, Germany). This tool, calibrated to provide actual acoustic intensity output levels corresponding to power settings of the single channel amplifier, allowed arbitrary sonication patterns with respect to burst count and duty cycle to be defined.

2.3.4. Experimental Setup

To evaluate the cell sonicator system's performance, we measured pressure distribution fields using an in-house constructed sound field scanner system. The cell sonicator was positioned in a cardanic support to ensure that its acoustic axis was aligned with the z-axis of the scanning system. A calibrated hydrophone (Type S, RP Acoustics, Leutenbach, Germany) mounted on a mechanical arm moveable in 3D was used to acquire the pressure signals. For the in-well characterization, the well plate was positioned on the various platforms, and sound pressure measurements were carried out in the individual wells using the hydrophone. The hydrophone was positioned in the middle of the individual wells and moved stepwise (100 µm steps) from the bottom to the top edge of the well (Figure 6). For each position in the scan field, the acoustic raw data were acquired, and stored in a custom data format, and relevant metrics were computed.

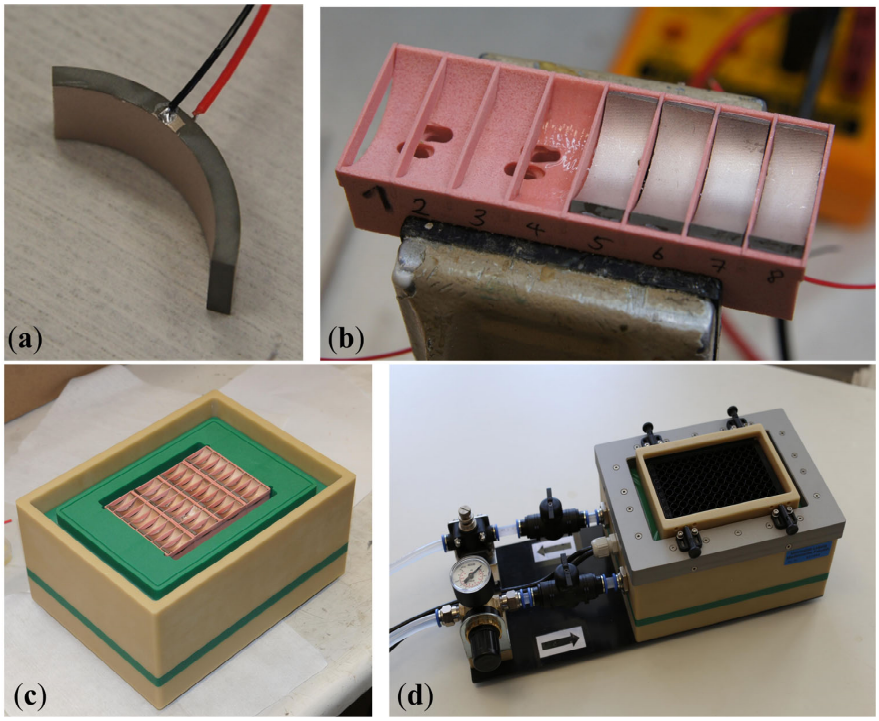

Figure 5. Setup of the HIFU system. (**a**) Single cylindrically focusing element of the 1 MHz HIFU applicator; (**b**) 8-element stack of elements mounted on an OBO backing with sound field separators between elements; (**c**) Integration of the 8 stacks into the housing; (**d**) Final integration of the 32 elements into the housing with the water cooling unit and a holder for a 96-well plate.

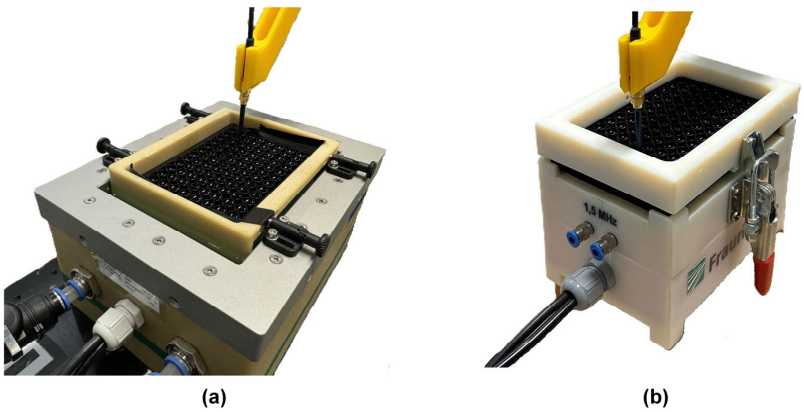

Figure 6. Setup of the in-well measurement with the hydrophone from the bottom to the top edge of the single well in 100 µm-steps (**a**) HIFU platform; (**b**) LIFU platform.

3. Results

In order to characterize the different platforms, the sound pressure distribution and the output homogeneity were investigated (Section 3.1). Another important aspect was to study the influence of the well plate itself (Section 3.2). Furthermore, the influence of the different filling volumes on the sound pressure values and their distribution was studied (Section 3.3). Another important aspect of the investigations was the measurement and analysis of the influence of sound application from one well to the neighboring ones (cross-coupling) (Section 3.4).

3.1. Ultrasound Sound Pressure Distribution and Output Homogeneity

3.1.1. LIFU Platform

The LIFU sonication device was characterized in four frequencies between 0.5 and 2.0 MHz with respect to homogeneity by measuring an xy-pressure field distribution 10 mm in front of the applicator, viewed on dB-scaled intensity maps (Figure 7a). All setups maintained the voltage applied to a single transducer at 25 V_{rms} by electrical adjustments. The maximum pressure output for each well position was extracted from the data to serve as a metric for qualitative assessment. Well center positions, defined based on the known well grid pitch and maximum pressure values within areas corresponding to the well floor (circles of 6.5 mm in diameter), were identified for each well position. For each frequency, the average effective pressure and the corresponding standard deviation were calculated (Figure 7b).

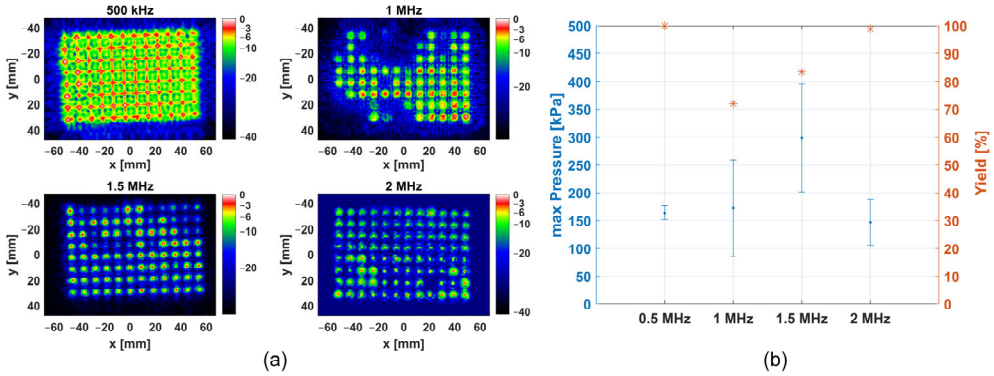

Figure 7. Homogeneity studies with the LIFU platform at frequencies between 0.5 and 2.0 MHz. (**a**) dB-scaled xy intensity distribution in front of the applicator (z = 10 mm) obtained through an xy-scan of a calibrated hydrophone; (**b**) Statistical assessment of the output homogeneity and the manufacturing yield for the different applicator versions.

When driven with 25 V_{rms}, the output pressure for all applicators ranged from 145 kPa to 300 kPa. The 0.5 MHz, 1 MHz, and 2.0 MHz models had an average output of around 160 kPa, while the 1.5 MHz model exceeded them with 300 kPa. The 0.5 MHz model presented the highest level of homogeneity with a relative standard deviation of 7%, while the other applicators varied between 27 and 51%. All applicators achieved a high yield of over 70%, defined as the number of elements whose output exceeded −6 dB of the average output pressure. Notably, the 500 kHz and 2 MHz models showed a very high yield, exceeding 95%, with minimal elements outside the −6 dB limit. To measure the impact of the excitation voltage on the maximum sound pressure and the intensity, the excitation voltage applied to the LIFU platform was varied between 6 and 48 V_{peak}. The filling volume in the wells was 250 µL. The maximum sound pressure amounted to 605 kPa (p_{max}) with maximum I_{SPPA} values between 0.78 and 12.38 W/cm^2 (Figure 8).

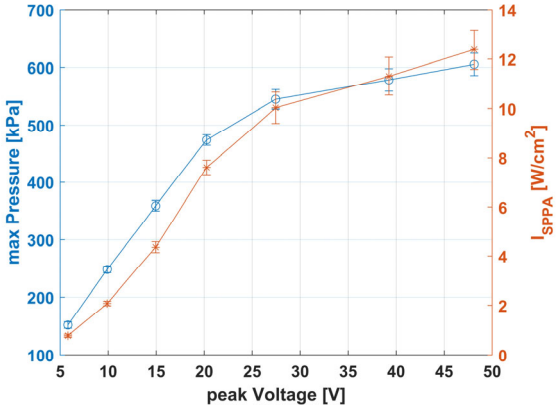

Figure 8. Single element output in terms of maximum pressure and I_{SPPA} as a function of the driving voltage (mean and standard deviation values of 4 elements) in the LIFU platform. Volume in well 250 µL.

3.1.2. HIFU Platform

The HIFU platform was characterized with respect to the emitted pressure distribution patterns, pressure amplitude, and output homogeneity across its 8 × 4 elements. The study first investigated the −6 dB pressure field width in the longitudinal and axial dimensions of an 8-element stack and the influence of the sound field separators between adjacent elements. Figure 9a–c compare the pressure distribution fields with and without the separation elements. The −6 dB width was reduced from 7.5 mm to 5.6 mm with the inclusion of the separation elements, ensuring the primary −6 dB field lobe remained within one well diameter of the 96-well plate. In the longitudinal direction, the focus was narrower with a −6 dB width of 1.4 mm (Figure 9c).

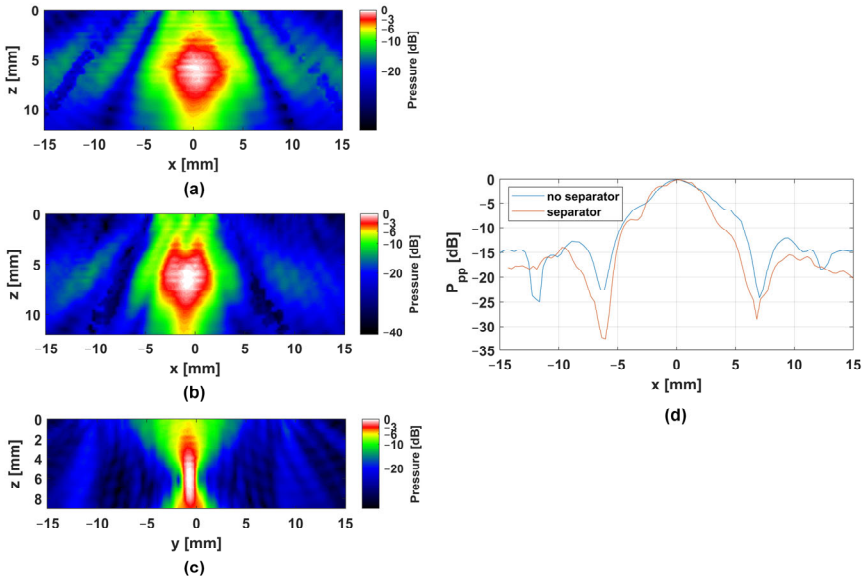

Figure 9. Lateral sound field (in the direction of an 8-element stack) without (**a**) and with (**b**) the inter-element separators. (**c**) Elevational sound field in the direction perpendicular to the stack; (**d**) Comparison of lateral pressure distribution fields with and without separators.

For the assessment of the homogeneity of acoustic output, an xy-scan was performed with an axial dimension corresponding to that of the well floor. Based on the known positions of the elements, the maximum pressure for each well position (Figure 10a) was extracted from the data. For statistical assessment of the applicator performance, the average output and standard deviation were calculated (Figure 10b). As with the LIFU

applicator models, yield was defined as the number of elements whose output was greater than −6 dB of the average output. Accordingly, the standard deviation of the applicator output was 19%, and the yield was 94%. The lowest element output was 41% of the average.

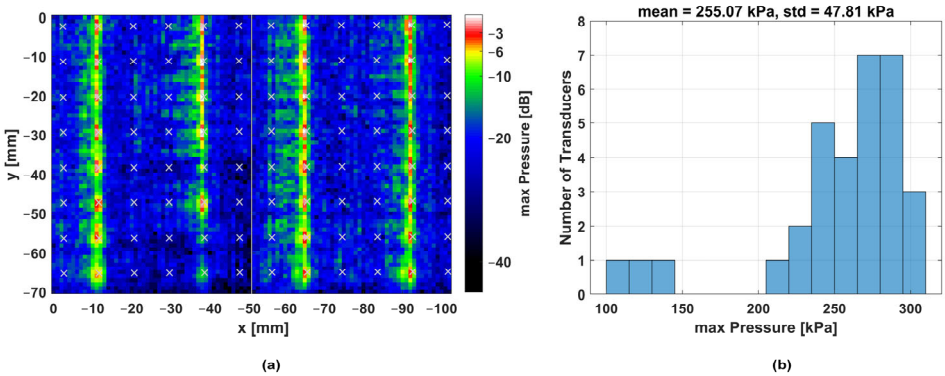

Figure 10. (**a**) dB scaled pressure distribution measured by a 2D scan of a calibrated hydrophone; The cross signs in the figure show the position of the individual wells. (**b**) Corresponding statistical analysis of applicator homogeneity.

The maximum focal pressure when driving the applicator with 94 V_{peak} was 1460 kPa (p_{max}) resulting in an I_{SPPA} of 72 W/cm^2 (Figure 11).

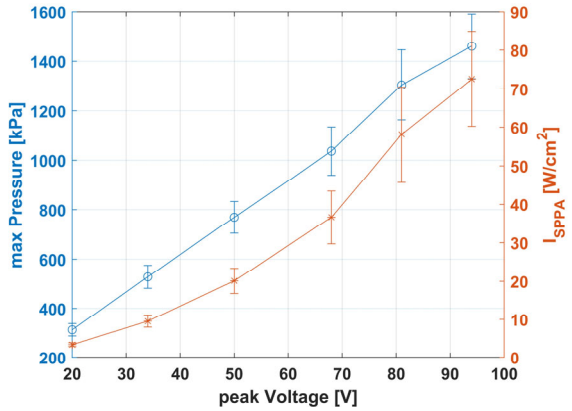

Figure 11. Single element output in terms of maximum pressure and I_{SPPA} as a function of the driving voltage (mean and standard deviation values for the 8 elements in row 8) in the HIFU platform. Volume in well 250 µL.

3.2. Influence of the Well Plate

A significant issue that was investigated in this study was the impact of the well plate on the sound pressure. In our experiments, a standard well plate with a membrane bottom of a minimal thickness (190 µm) was used (Greiner Bio-One, Kremsmünster, Austria, type µClear®, item no. 655090).

Sound pressure measurements were conducted with the hydrophone in 32 wells and compared with the free-field measurements at precisely the same locations. The investigations were conducted with the high-intensity focused ultrasound (HIFU) platform, operating at a center frequency of 1 MHz, due to its minimal dependence on filling volume resulting from its pronounced focusing at approximately 2 mm (for further details see Section 3.3.2).

In the free-field measurements carried out without the presence of a well plate, the maximum sound pressure was observed to be 255 kPa on average when driven with a voltage of V_{peak} = 20 V. At the same excitation voltage, a sound pressure of approximately 200–240 kPa (standard deviation of 40–54 kPa) was measured in the wells (dependent on

the filling volume, between 200 µL and 350 µL). The results indicated that the impact of the well plate, contingent upon the filling volume, ranged between −2.2 and −0.6 dB of attenuation, representing a minimal influence.

3.3. Influence of Filling Volume

The findings of the investigation indicated that there is a notable relationship between the filling volume in the wells and the sound pressures generated within them. In order to gain further insight into this relationship, the investigation was conducted on the two different platforms.

3.3.1. LIFU Platform

In the course of the investigation into the influence of the filling volumes on the sound pressure in the individual wells, the 1.5 MHz version of the LIFU platforms was used. The measurements were conducted with varying filling volumes per well (200 µL, 250 µL, 300 µL, 350 µL) and at distinct positions within 48 individual wells. A z-line was measured in each of the wells in the direction of radiation, starting at a distance of 1 mm from the bottom of the wells and continuing up to a height of 10 mm. The step size of the measurements was 0.1 mm. Figure 12 illustrates the results of such a measurement in one representative well.

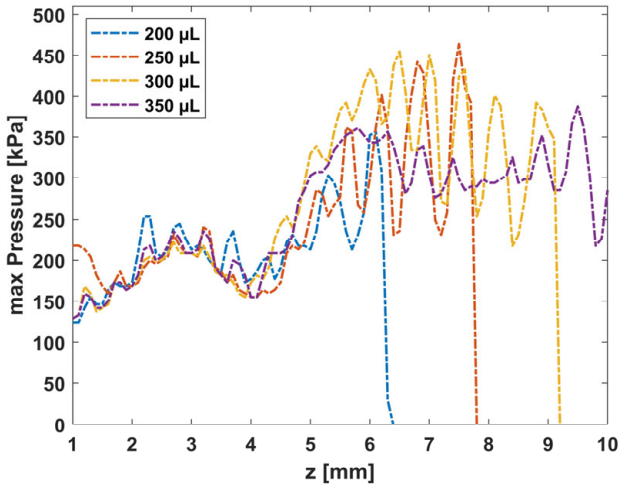

Figure 12. Results of hydrophone measurements with the 1.5 MHz LIFU platform along the z-axis in a representative well (no. 21) of a 96-well plate from the bottom of the well (z = 1 mm) to the maximum filling level at the different filling volumes (200 µL, 250 µL, 300 µL, 350 µL). The step size of the measuring positions along the z-axis was 0.1 mm.

The results of the study indicated a considerable influence of both the filling volume on the maximum sound pressure and on the axial position of the sound pressure maximum in the well (Figure 13). The results of the maximum sound pressures (p_{max}) for the individual filling volumes are presented in Table 2. These results demonstrated a variation in maximum sound pressure between 244 kPa (standard deviation 106 kPa) for a 200 µL filling volume and 294 kPa (standard deviation 107 kPa) for a 350 µL filling volume when driven with a voltage of 15 V_{peak}. Additionally, the data illustrate a strong variability in the position of maximum sound pressure within the well, with values ranging between 6 and 9 mm, highlighting the impact of the filling volume and of the transducer sound field characteristics.

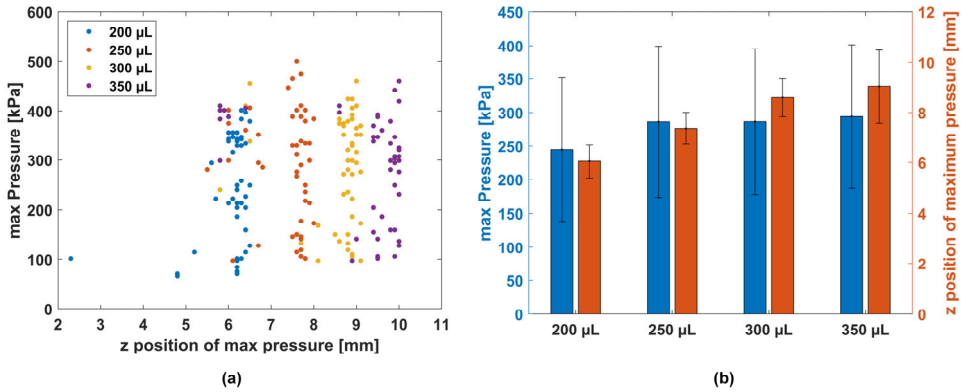

Figure 13. Results of hydrophone measurements with the 1.5 MHz LIFU platform. The ratio of filling volume and measuring position in the well along the z-axis in the 48 wells from the bottom of the well (z = 1 mm) to the maximum filling level at the different filling volumes (200 µL, 250 µL, 300 µL, 350 µL) was analyzed. The step size along the z-axis was 0.1 mm. The influence of the filling volume on the maximum pressure and position of maximum pressure from measurements was analysed in 48 single wells. (**a**) Data are presented as a scatter plot. (**b**) Data are presented as a bar diagram, including mean value and SD.

Table 2. Maximum sound pressure levels in the 48 wells at different filling volumes and positions within the wells.

	200 µL	**250 µL**	**300 µL**	**350 µL**
mean p_{max} [kPa]	244.78	286.35	286.65	294.20
SD p_{max} [kPa]	106.70	112.96	108.78	107.15
mean z_{pos} [mm]	6.05	7.38	8.59	9.04
SD z_{pos} [mm]	0.66	0.63	0.75	1.46

p_{max} = maximum pressure, z_{pos} = z-position of maximum pressure, SD = standard deviation.

3.3.2. HIFU Platform

The same measurements were conducted to examine the influence of the filling volumes on the sound pressure in the individual wells, this time for the HIFU platform (1 MHz). The scan settings were identical to the LIFU case (Filling 200–350 µL, z-scan from 1 mm to 10 mm in 0.1 mm steps). Figure 14 illustrates the results of these measurements.

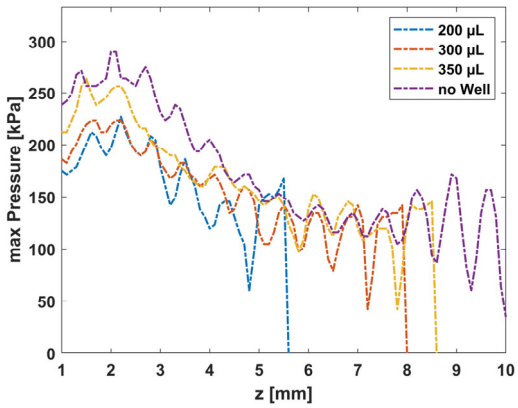

Figure 14. Results of hydrophone measurements with the 1 MHz HIFU platform along the z-axis in a representative well of a 96-well plate. Measurements were taken from the bottom of the well (z = 1 mm) to the maximum filling level for the different filling volumes (200 µL, 300 µL, 350 µL). Additional free-field measurements were performed at identical positions (no well). The step size along the z-axis was 0.1 mm.

The results of this investigation, as illustrated in Figure 15, demonstrated the impact of varying filling volumes on sound pressure levels across 32 distinct wells. The results of the maximum sound pressure (p_{max}) when driven with a voltage of V_{peak} 20 V for the individual filling volumes are presented in Table 3. The observed variation ranged from 197 kPa (SD 40 kPa) for 200 µL to 255 kPa (SD 47 kPa) for 350 µL filling. The results of the HIFU platform indicated that the influence of different filling volumes in the well was minimal. The axial positions at which the maximum sound pressures were measured were approximately the same for all filling volumes, varying only between 2.36 (200 µL) and 2.14 mm (350 µL). Furthermore, these values differed only marginally from the measurements taken without the well plate.

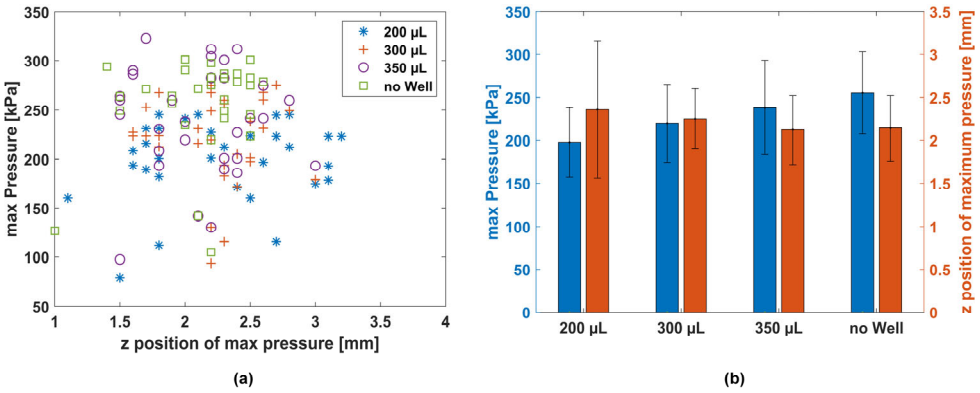

Figure 15. Results of hydrophone measurements with the 1 MHz HIFU platform. A correlation between filling volume and measuring position in the well with the HIFU platform (1 MHz) along the z-axis in the 32 wells from the bottom of the well (z = 1 mm) to the maximum filling level at the different filling volumes (200 µL, 300 µL, 350 µL) was analyzed. The step size along the z-axis was 0.1 mm. The influence of filling volume and measuring position on the position of the maximum sound pressure level from measurements was analysed in 32 single wells. (**a**) Data are presented as a scatter plot. (**b**) Data are presented as a bar diagram, including mean value and SD.

Table 3. Maximum sound pressure levels in the 32 wells at different filling volumes and positions within the wells.

	200 µL	**300 µL**	**350 µL**	**No Well**
mean p_{max} [kPa]	197.66	219.82	238.19	255.07
SD p_{max} [kPa]	40.60	45.14	54.70	47.81
mean z_{pos} [mm]	2.36	2.25	2.12	2.14
SD z_{pos} [mm]	0.80	0.35	0.40	0.38

p_{max} = maximum pressure, z_{pos} = z-position of maximum pressure, SD = standard deviation.

The results of these investigations demonstrated that the sound pressure distribution within the well was almost independent of the water filling volume, in contrast to the LIFU platform, which was only capable of natural focusing.

3.4. Cross-Coupling Between the Wells (HIFU)

It is also important to consider the effect of sound propagation from the active wells to the adjacent well when using these platforms or similar setups on standard multi-well plates. It is therefore essential to minimize the impact of this cross-talk in order to accurately determine the sound intensity and sound pressure acting on the media within the well. In order to investigate this influence, the HIFU platform was employed. In this configuration, only four rows (32 transducers) were active, while two adjacent rows were not sonicated. The maximum sound pressure was measured in all wells of the 96-well

plate, and the cross-talk to inactive wells was determined using a hydrophone positioned within each individual well. The acoustic pressure values along the z-axis in each well (96) were recorded with a step size of 0.1 mm, from the bottom of the well (z = 1 mm) to the maximum filling height of 10 mm at a filling volume of 350 µL. The platform was operated with an excitation voltage of V_{peak} 20 V.

The maximum sound pressure levels were observed to range between 204 kPa (SD 17 kPa) and 290 kPa (SD 22 kPa) in the activated transducer positioned beneath the wells of rows 2, 5, 8, and 11. In the non-sonicated wells, the maximum sound pressure levels were observed to be between 19 kPa (SD 4.8 kPa) and 31 kPa (SD 4.8 kPa) (Figure 16).

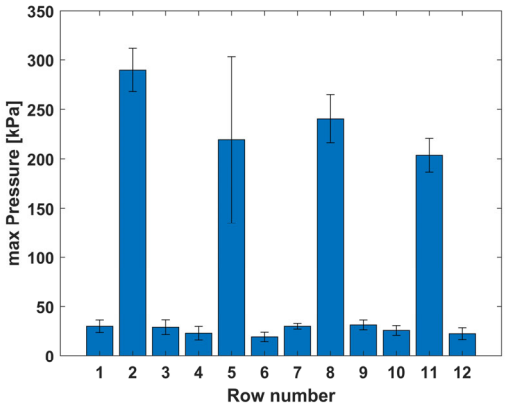

Figure 16. Results of the maximum sound pressure with the 1 MHz HIFU platform along the z-axis in each well (96) from the bottom of the well (z = 1 mm) to the maximum filling height of 10 mm at a filling volume of 350 µL. Thirty-two wells (4 rows of 8 wells each) were exposed to ultrasound.

The measured values demonstrated that the cross-coupling in this HIFU platform did not exceed 13% of the mean sound pressure. Consequently, a sound pressure that was attenuated only by a maximum of −18 dB was applied to the surrounding wells. The values of these measurements can be employed to calculate the precise applied sound pressure per well when utilizing such a platform.

4. Discussion

During this study, an HTP platform for parallel cell sonication optimized for in vitro workflows based on multi-well plates was successfully developed. Traditional cell culture sonication setups are mostly based on single ultrasound transducers mechanically maneuvered below the well plate [16–22]. Our design enabled parallel sonication enhancing experimental workflow speed. However, handling data from many transducers in parallel presents challenges. For scenarios, like those using piston-like non-focusing transducers in the LIFU applicator model, we adopted parallel milling of 96 elements from a singular piezo composite plate. Although efficient, this fabrication method limited control over the homogeneity and yield of the applicator since defective elements were irreplaceable after characterization. In the LIFU model, this resulted in an element output standard deviation from 7 to 51% and yields from 70 to 100%. The inconsistent readings of homogeneity across LIFU models may arise from using bulk PZT or piezo composites and different milling parameters, warranting further investigation. In addition, the results showed that limiting the diameter of the ultrasonic transducer elements to the well diameter was ineffective for higher frequencies (>1 MHz). The natural focus with the maximum intensity was laterally located in the well diameter but was too far away in the direction of beam emission.

In contrast, the HIFU model demonstrated improved performance with a consistent 94% yield and greater homogeneity with a 19% standard deviation of the acoustic power, which however comes at the price of a more complex assembly. When aiming for an

optimal homogeneity in the LIFU setup, a method similar to that of the HIFU applicator is recommended, with the elements mounted on a support with individual electrical contacts in an easily serviceable configuration.

We aimed to develop versatile, easy-to-operate tools for sonication over a wide range of parameters, both in terms of frequencies and applied intensities. Depending on the diameter-to-thickness ratio and the corresponding material vibration modes, we selected either bulk PZT or piezo composite, allowing for efficient operation. With the dry-coupling approach, we observed that the heating of the material when operating the device at duty cycles greater than 5%. Accordingly, we built the HIFU version with cylindrically shaped transducers immersed in a stream of water, ensuring heat dissipation and allowing the transducers to operate at 100% of the DC supply. The difference in allowed duty cycles together with the achievable pressures, led to maximum I_{SPPA} values between 0.78 and 12.38 W/cm^2 for the LIFU version (1.5 MHz) and 72 W/cm^2 for the HIFU version, respectively.

Importantly, our models achieved efficient confinement of acoustic energy to the wells. The lateral spread of the pressure distribution fields (-6 dB width) was less than the 6.5 mm diameter of the well in the case of a 96-well plate. Achieving this presented a greater challenge in the HIFU model where the free field -6 dB width was greater than 7 mm. We were able to reduce it to 5.6 mm by using separation elements between the individual transducers. The HIFU model allowed the sonication of 32 wells simultaneously, enabling the treatment of each well of a 96-well plate with only three repositioning steps of the plate. To ensure the most efficient application of the ultrasonic waves and minimize loss within the wells, a well plate with a minimal bottom thickness was utilized. The results of our investigation demonstrated that the attenuation of the maximum sound pressure values when propagating through the well plate was minimal, with a reduction of -2.2 dB at 200 µL and -0.6 dB at 350 µL, in comparison to the free-field measurement. Additionally, it was observed that the distribution of sound pressure within the wells was affected by variations in filling height. The recorded values ranged from 244 kPa (SD 106 kPa) for a 200 µL filling volume to 294 kPa (SD 107 kPa) for a 350 µL filling volume.

Furthermore, it was determined that the positions of maximum sound pressure in the LIFU setup showed variability, ranging between 6 mm and 9 mm. This is attributable to the absence of focusing in the well. This means that the filling level in each well has to be taken into account when calibrating the applicator. In contrast, the HIFU setup demonstrated a relatively lower dependence on the filling volume. The recorded values ranged from 197 kPa (SD 40 kPa) for 200 µL to 255 kPa (SD 47 kPa) for 350 µL filling. Furthermore, due to the strong focusing in the well, the position of the maximum sound pressure showed only a slight variation of approximately 0.2 mm.

It is also crucial to consider the cross-coupling of ultrasound between neighboring wells when utilizing such platforms. If this is not sufficiently considered, the investigations conducted with these platforms may be based on erroneous values of the applied sound pressure and intensity.

In this study, we demonstrated that by employing the HIFU version and integrating specific separators between the ultrasonic transducers, the cross-coupling from the active well to neighboring wells could be reduced to a value of -18 dB.

5. Conclusions

In this work, we implemented and characterized two versions (LIFU and HIFU) of cell sonication devices that enable standardization of in vitro workflows for HTP investigations by parallelized sonication. The wide intensity and frequency bandwidths allowed an effective exploration of the fundamental mechanisms of the action of therapeutic ultrasound on a wide variety of in vitro models in preclinical research.

In conclusion, different cell sonication tools optimized for 96-well plates were developed. The LIFU and HIFU versions have different advantages and limitations. The manufacturing process of the HIFU applicator based on individual transducers allows a preselection prior to integration, which, in the end, allows a higher yield and homogeneity. Furthermore, the implementation of a water-cooling system ensures that the sonicated samples are not subjected to heating by the transducer surface, thereby preventing any adverse effects. In addition, the cooling allows driving the transducers at duty cycles up to 100%. However, the risk of air bubbles trapped below the membrane is a side effect of water cooling, which must be considered. Finally, the limitation of sonication to only 32 of the 96 wells in parallel, which resulted in the use of focusing transducers with a footprint larger than the well-to-well distance, is a notable drawback of this setup. On the other hand, the main advantage of the LIFU variant is the capability for dry coupling, eliminating the risk of air bubbles and making the use more convenient. Providing access to all 96 wells furthermore makes it easier to achieve statistical significance when investigating therapeutic effects in vitro.

Future work could focus on a combination of the two versions. For instance, a system with individually manufactured transducers integrated into standard housings would allow the preselection of a highly homogeneous subset of transducers and the integration of arbitrary transducer combinations (e.g., of different frequencies) in the same multi-well applicator. Such screwable and interchangeable transducers would not only increase flexibility but improve maintenance in case of transducer defects. In addition, ultrasonic transducers could be equipped with a customized acoustic lens to optimize focusing in the wells and to adapt the focus spot size better to the well geometry (or to some inserts, e.g., when using membrane models for BBB opening). Finally, it would be beneficial to equip the transducer elements with temperature sensors to facilitate temperature-controlled application and, thereby, ensure that the observed effects actually result from an acoustic effect in the cell medium and not from thermal diffusion.

The potential for future integration of electronics with 96 transmission channels could also be explored. This could enhance the individualization of the sound output in each well, allowing for precise control over frequency, intensity, and transmission signal sequences.

In a recent study, the potential of our cell sonication setup for investigation of tumor spheroids treatment was demonstrated [26]. The researchers showed that low-intensity pulsed-focused ultrasound reduced spheroid growth metabolic activity and increased DNA double-strand breaks in in vitro cancer cell models. Our future work will aim at developing multichannel electronics and adapted ultrasonic transducers to meet the great need for technologies for investigating the mode of action of ultrasound on biological cells and cellular networks as pre-studies for more efficient application of ultrasound in future therapies.

Author Contributions: Conceptualization, S.H.T.; methodology, S.H.T., C.D., F.-J.B. and P.W.; software, S.H.T. and W.B.; validation, S.H.T., M.F., F.-J.B., W.B., L.L. and A.M.; formal analysis, S.H.T., M.F., W.B. and S.T.-M.; investigation, S.H.T., M.F., C.D., F.-J.B., P.W., W.B., L.L. and A.M.; resources, S.H.T. and A.M.; data curation, S.H.T., M.F., W.B., L.L. and S.T.-M.; writing—original draft preparation, S.H.T.; writing—review and editing, S.H.T., M.F., C.D., F.-J.B., P.W., W.B., L.L., S.T.-M. and A.M.; visualization, S.H.T., M.F., W.B. and S.T.-M.; supervision, A.M.; project administration, S.H.T. and A.M.; funding acquisition, A.M. All authors have read and agreed to the published version of the manuscript.

Funding: This research was funded by the Federal Ministry for Education and Research (BMBF), grant number 03Z1L511 (SONO-RAY).

Institutional Review Board Statement: Not applicable.

Informed Consent Statement: Not applicable.

Data Availability Statement: Data are contained within the article.

Acknowledgments: The authors thank Will Strokes, University of Leeds, United Kingdom, for proofreading and the Federal Ministry of Education and Research (BMBF) for funding.

Conflicts of Interest: The authors declare no conflicts of interest.

References

1. White, E.; Broad, M.; Myhre, S.; Serafini, M.R.; Chesnut, A.; Browning, M.; Heishman, D.; Knupp, J.; Andreae, T.; Chao, J.C. *2022 State of the Field Report*; Focused Ultrasound Foundation: Charlottesville, VA, USA, 2022; pp. 1–340.
2. Anneveldt, K.J.; van't Oever, H.J.; Nijholt, I.M.; Dijkstra, J.R.; Hehenkamp, W.J.; Veersema, S.; Huirne, J.A.F.; Schutte, J.M.; Boomsma, M.F. Systematic review of reproductive outcomes after High Intensity Focused Ultrasound treatment of uterine fibroids. *Eur. J. Radiol.* **2021**, *141*, 109801. [CrossRef] [PubMed]
3. Sofuni, A.; Asai, Y.; Mukai, S.; Yamamoto, K.; Itoi, T. High-intensity focused ultrasound therapy for pancreatic cancer. *J. Med. Ultrason.* **2022**. [CrossRef]
4. Dupré, A.; Melodelima, D.; Cilleros, C.; De Crignis, L.; Peyrat, P.; Vincenot, J.; Rivoire, M. High Intensity Focused Ultrasound (HIFU) in Digestive Diseases: An Overview of Clinical Applications for Liver and Pancreatic Tumors. *IRBM* **2023**, *44*, 100738. [CrossRef]
5. Meng, Y.; Hynynen, K.; Lipsman, N. Applications of focused ultrasound in the brain: From thermoablation to drug delivery. *Nat. Rev. Neurol.* **2021**, *17*, 7–22. [CrossRef]
6. Darrow, D.P. Focused Ultrasound for Neuromodulation. *Neurotherapeutics* **2019**, *16*, 88–99. [CrossRef]
7. Bubrick, E.J.; McDannold, N.J.; White, P.J. Low Intensity Focused Ultrasound for Epilepsy—A New Approach to Neuromodulation. *Epilepsy Curr.* **2022**, *22*, 156–160. [CrossRef]
8. Moosa, S.; Martínez-Fernández, R.; Elias, W.J.; Del Alamo, M.; Eisenberg, H.M.; Fishman, P.S. The role of high-intensity focused ultrasound as a symptomatic treatment for Parkinson's disease. *Mov. Disord.* **2019**, *34*, 1243–1251. [CrossRef]
9. Shah, B.R.; Lehman, V.T.; Kaufmann, T.J.; Blezek, D.; Waugh, J.; Imphean, D.; Yu, F.F.; Patel, T.R.; Chitnis, S.; Dewey, R.B.; et al. Advanced MRI techniques for transcranial high intensity focused ultrasound targeting. *Brain* **2020**, *143*, 2664–2672. [CrossRef]
10. Nüssel, M.; Zhao, Y.; Knorr, C.; Regensburger, M.; Stadlbauer, A.; Buchfelder, M.; Del Vecchio, A.; Kinfe, T. Deep Brain Stimulation, Stereotactic Radiosurgery and High-Intensity Focused Ultrasound Targeting the Limbic Pain Matrix: A Comprehensive Review. *Pain Ther.* **2022**, *11*, 459–476. [CrossRef]
11. Yuksel, M.M.; Sun, S.; Latchoumane, C.; Bloch, J.; Courtine, G.; Raffin, E.E.; Hummel, F.C. Low-Intensity Focused Ultrasound Neuromodulation for Stroke Recovery: A Novel Deep Brain Stimulation Approach for Neurorehabilitation? *IEEE Open J. Eng. Med. Biol.* **2023**, *5*, 300–318. [CrossRef]
12. Zafar, A.; Quadri, S.A.; Farooqui, M.; Ortega-Gutiérrez, S.; Hariri, O.R.; Zulfiqar, M.; Ikram, A.; Khan, M.A.; Suriya, S.S.; Nunez-Gonzalez, J.R.; et al. MRI-Guided High-Intensity Focused Ultrasound as an Emerging Therapy for Stroke: A Review. *J. Neuroimaging* **2019**, *29*, 5–13. [CrossRef] [PubMed]
13. Leinenga, G.; Langton, C.; Nisbet, R.; Götz, J. Ultrasound treatment of neurological diseases--current and emerging applications. *Nat. Rev. Neurol.* **2016**, *12*, 161–174. [CrossRef] [PubMed]
14. Stewart, F.; Cox, B.F.; Wang, G.; Huang, Z.; Newton, I.P.; Nathke, I.S.; Thanou, M.; Cochran, S. An in vitro sonication system for applications in ultrasound-mediated targeted drug delivery. In Proceedings of the 2016 IEEE International Ultrasonics Symposium (IUS), Tours, France, 18–21 September 2016; pp. 1–4. [CrossRef]
15. De Oliveira, P.D.; de Almeida Pires-Oliveira, D.A.; Dragonetti Bertin, L.; Fernandes Szezerbaty, S.K.; de Oliveira, R.F. The effect of therapeutic ultrasound on fibroblast cells in vitro: The systematic review. *Arch. Med. Deporte* **2018**, *35*, 50–55.
16. Doan, N.; Reher, P.; Meghji, S.; Harris, M. In vitro effects of therapeutic ultrasound on cell proliferation, protein synthesis, and cytokine production by human fibroblasts, osteoblasts, and monocytes. *J. Oral Maxillofac. Surg.* **1999**, *57*, 409–419. [CrossRef]
17. Patel, U.S.; Ghorayeb, S.R.; Yamashita, Y.; Atanda, F.; Walmsley, A.D.; Scheven, B.A. Ultrasound field characterization and bioeffects in multiwell culture plates. *J. Ther. Ultrasound* **2015**, *30*, 8. [CrossRef]
18. Secomski, W.; Bilmin, K.; Kujawska, T.; Nowicki, A.; Grieb, P.; Lewin, P.A. In vitro ultrasound experiments: Standing wave and multiple reflections influence on the outcome. *Ultrasonics* **2017**, *77*, 203–213. [CrossRef]
19. Zhang, X.; Bobeica, M.; Unger, M.; Bednarz, A.; Gerold, B.; Patties, I.; Melzer, A.; Landgraf, L. Focused ultrasound radiosensitizes human cancer cells by enhancement of DNA damage. *Strahlenther Onkol.* **2021**, *197*, 730–743. [CrossRef]
20. Crapps, J.; Rahimi, A.; Case, N. Analysis of a novel bioreactor designed for ultrasound stimulation of cell-seeded scaffolds. In Proceedings of the 2018 IEEE International Symposium on Signal Processing and Information Technology (ISSPIT), Louisville, KY, USA, 6–8 December 2019; pp. 1–6. [CrossRef]

21. Nakao, M.; Imashiro, C.; Kuribara, T.; Kurashina, Y.; Titani, K.; Takemura, K. Formation of Large Scaffold-Free 3-D Aggregates in a Cell Culture Dish by Ultrasound Standing Wave Trapping. *Ultrasound Med. Biol.* **2019**, *45*, 1306–1315. [CrossRef]
22. Gourevich, D.; Hertzberg, Y.; Volovick, A.; Shafran, Y.; Navon, G.; Cochran, S.; Melzer, A. Ultrasound-mediated targeted drug delivery generated by multifocal beam patterns: An in vitro study. *Ultrasound Med. Biol.* **2013**, *39*, 507–514. [CrossRef]
23. Puts, R.; Ruschke, K.; Ambrosi, T.H.; Kadow-Romacker, A.; Knaus, P.; Jenderka, K.-V. A focused low-intensity pulsed ultrasound (FLIPUS) system for cell stimulation: Physical and biological proof of principle. *IEEE Trans. Ultrason. Ferroelectr. Freq. Control* **2016**, *63*, 91–100. [CrossRef]
24. Louw, T.M.; Subramanian, A.; Viljoen, H.J. Theoretical evaluation of the acoustic field in an ultrasonic bioreactor. *Ultrasound Med. Biol.* **2015**, *41*, 1766–1778. [CrossRef] [PubMed]
25. Leskinen, J.J.; Hynynen, K. Study of Factors Affecting the Magnitude and Nature of Ultrasound Exposure with In Vitro Set-Ups. *Ultrasound Med. Biol.* **2012**, *38*, 777–794. [CrossRef] [PubMed]
26. Landgraf, L.; Kozlowski, A.; Zhang, X.; Fournelle, M.; Becker, F.J.; Tretbar, S.; Melzer, A. Focused Ultrasound Treatment of a Spheroid In Vitro Tumour Model. *Cells* **2022**, *11*, 1518. [CrossRef]